Interaction Kinetics of Tetramethylrhodamine Transferrin with Human Transferrin Receptor Studied by Fluorescence Correlation Spectroscopy

Jens Schüler,[‡] Joachim Frank,[‡] Ulrike Trier,[§] Monika Schäfer-Korting,[§] and Wolfram Saenger*[,‡]

Institut für Kristallographie, Freie Universität Berlin, Takustrasse 6, D-14195 Berlin, Germany, and Institut für Pharmazie II, Abteilung für Pharmakologie und Toxikologie, Freie Universität Berlin, Königin-Luise-Strasse 2-4, D-14195 Berlin, Germany

Received August 13, 1998; Revised Manuscript Received April 2, 1999

ABSTRACT: We applied fluorescence correlation spectroscopy (FCS) to characterize the interaction dynamics of fluorescence-labeled transferrin with transferrin receptor (hTfR) associates isolated from human placenta. The dissociation constant for the equilibrium binding of TMR-labeled ferri-transferrin to hTfR in detergent free solution was determined to be 7 ± 3 nM. Binding curves were compatible with equal and independent binding sites present on the hTfR associates. Under pseudo-first-order conditions, with respect to transferrin, complex formation is monophasic. From these curves, association and dissociation rate constants for a reversible bimolecular binding reaction were determined, with $(1.1 \pm 0.1) \times 10^4$ M^{-1} s^{-1} for the former and $(6 \pm 4) \times 10^{-4}$ s^{-1} for the latter. In dissociation exchange experiments, biphasic curves and concentration-independent reciprocal relaxation times were determined. From isothermal titration calorimetry experiments, we obtained an enthalpy change of −44.4 kJ/mol associated with the reaction. We thus conclude that the reaction is mainly enthalpy driven.

Human transferrin receptor is a class II transmembrane glycoprotein (*1*). It is composed of two identical subunits, with a molecular mass of 90−95 kDa each (*2*, *3*). The subunits are linked by a disulfide bond, such that the major part of the molecule is exposed to the cell surface. Each subunit consists of a 61-residue cytoplasmic domain, a 28-residue membrane-spanning region made up of hydrophobic amino acids, and a 760-residue extracellular domain with three N-glycosylation sites and one O-glycosylation site (*4*). Each subunit possesses one transferrin binding site in the extracellular domain (*3*, *5*). In vertebrate cells, hTfR[1] mediates the iron uptake by binding and internalization of the iron transport protein transferrin, in its diferric state (ferri-transferrin). Upon endocytosis, the hTfR−transferrin complex becomes exposed to an acidic pH in the endosome. Under this condition, the Fe^{3+} ions dissociate from the receptor-bound transferrin and are transported into the cytosol. The receptor−transferrin complex recycles back to the cell surface, where the iron free transferrin dissociates and is replaced by an iron-loaded one.

In detergent free solution, hTfR forms rosette-like structures made up of 8−12 hTfR dimers (*6*), with an apparent hydrodynamic radius of 16 nm (J. Schüler et al., unpublished experiments).

In previous equilibrium binding studies of the binding of transferrin (Tf) to hTfR, very different dissociation constants were obtained, depending on the experimental conditions. The dissociation constants determined for the binding of Tf to whole cells vary between 20 and 29 nM (*7*). For various cell extracts, values between 0.12 and 1.1 nM were reported (*8*−*10*). In a recent study with purified hTfR, a dissociation constant of 5 nM was determined (*11*).

To investigate the kinetics and equilibrium binding of ferri-transferrin to purified human transferrin receptor (hTfR), we measured the rates and degree of saturation for the binding of tetramethylrhodamine-labeled ferri-transferrin to hTfR using fluorescence correlation spectroscopy (FCS). During a FCS experiment, a sharply focused laser beam passes through a very small volume element ($0.2-1 \times 10^{-15}$ L). At any given point in time, there are only a few (one to five) fluorescent particles in this volume. The particles undergo Brownian motion, resulting in a time-dependent fluctuation of the fluorescence signal which can be analyzed in terms of an autocorrelation function, yielding translational diffusion times (τ_{diff}) for the fluorescent species that are present. The relative amount of each species can be obtained from the autocorrelation function, providing that their molecular masses are sufficiently different. In this paper, we will only give a very basic introduction to FCS, mainly based on user information provided by EVOTEC GmbH (Hamburg, Germany) (*12*). A detailed description of the underlying theory and possible experimental applications can be found elsewhere (*13*−*18*).

EXPERIMENTAL PROCEDURES

CNBr Sepharose and Sephacryl S-400 were purchased from Pharmacia. Desferral, human ferri-transferrin, and Triton X-100 were obtained from Sigma. All other salts and

* Corresponding author. Phone: +49-30-838-3412. Fax: +49-30-838-6702. E-mail: saenger@chemie.fu-berlin.de.

[‡] Institut für Kristallographie, Freie Universität Berlin.

[§] Institut für Pharmazie II, Abteilung für Pharmakologie und Toxikologie, Freie Universität Berlin.

[1] Abbreviations: hTfR, human transferrin receptor; Tf, transferrin; TMR-Tf, TMR-labeled transferrin; TMR, tetramethylrhodamine; PBS, phosphate-buffered saline [150 mM NaCl and 10 mM sodium phosphate (pH 7.5)]; CHAPS, 3-[(3-cholamidopropyl)dimethylammonio]-1-propanesulfonate; HEPES, [4-(2-hydroxyethyl)piperazino]ethanesulfonic acid; FCS, fluorescence correlation spectroscopy; ITC, isothermal titration calorimetry.

10.1021/bi9819576 CCC: $18.00
Published on Web 06/12/1999

buffer components were from Merck. All these substances were used without further purification.

TMR (tetramethylrhodamine; T-490) and human TMR transferrin (T-2872) were from Molecular Probes Europe (Leiden, The Netherlands). The molar ratio of dye to transferrin was 1.9 for TMR transferrin, according to the specification given by Molecular Probes. The fluorescence-labeled human transferrins were purified as described below.

hTfR was purified from human placenta according to Turkewitz et al. (*1*) with the following modifications. After removal of Fe^{3+} from the affinity column by 0.2 mM Desferral at pH 5.0, hTfR was eluted under nondenaturing conditions with 2 M KCl and 10 mM CHAPS in 50 mM HEPES (pH 7.5). Upon elution, CHAPS was removed by extensive dialysis against PBS (pH 7.5). The purity of the receptor was monitored by SDS−PAGE. To remove higher aggregates [hydrodynamic radius (R_h) of approximately 100 nm], the protein solution was further purified by gel filtration using a Sephacryl S-400 column.

The labeled transferrins still contain free dye. This was removed by passing the solution five times over a PD-10 column (Pharmacia). After each pass, the solution was concentrated using an Ultrafree-4 Centrifugal Filter Unit (Millipore) with a 30 kDa molecular mass cutoff. After purification, the free dye concentration of TMR-Tf was <5% (particle number).

All protein concentrations were determined using the Pierce BCA protein assay (Rockford, IL). We calculated the concentration of binding sites, assuming a molecular mass of 95 kDa for each subunit, considering that each subunit has one binding site for Tf (*3*, *5*).

Fluorescence Correlation Spectroscopy (FCS)

Theoretical Considerations. For a reversible bimolecular reaction of a labeled small ligand (A*) and a receptor (B):

$$\mathrm{A^*} + \mathrm{B} \underset{k_{-1}}{\overset{k_{+1}}{\rightleftharpoons}} \mathrm{A^*B}$$

the autocorrelation function, $G(\tau)$, can be expressed in terms of a two-component model according to eq 1 (*19*). Evaluation of the autocorrelation curves was carried out using a Marquardt nonlinear least-squares fitting routine, as implemented in the program FCS Access 2.0 (EVOTEC GmbH), using the following two-component model corresponding to free and bound labeled transferrin

$$G(\tau) = \left[1 - T + T\exp\left(\frac{-\tau}{\tau_T}\right)\right] N^{-1} \left[\frac{1-Y}{\left(1+\frac{\tau}{\tau_{\mathrm{free}}}\right)\sqrt{1+\frac{r_0^{\,2}}{z_0^{\,2}}\frac{\tau}{\tau_{\mathrm{free}}}}} + \frac{Y}{\left(1+\frac{\tau}{\tau_{\mathrm{bound}}}\right)\sqrt{1+\frac{r_0^{\,2}}{z_0^{\,2}}\frac{\tau}{\tau_{\mathrm{bound}}}}}\right] \quad (1)$$

with

$$Y = \frac{[\mathrm{A^*B}]}{[\mathrm{A^*}] + [\mathrm{A^*B}]}$$

where T is the average fraction of dye molecules in the triplet state with relaxation time τ_T, N is the total average number of fluorescent molecules in the observation volume, Y is the relative concentration fraction of bound A*, τ_{free} and τ_{bound} define the average time (diffusion time) for detected molecules of free and bound A*, respectively, and r_0 and z_0 are the lateral and axial distances, respectively, between the coordinate where the Gaussian emission light distribution adopts the maximum value and the point where the light intensity decreases down to $1/e^2$ of the maximum value (observation volume). Lateral and axial lengths of the observation volume are related through the structure parameter SP:

$$z_0 = r_0 \mathrm{SP} \quad (2)$$

To obtain r_0, the translational diffusion time, τ_{diff}, of a standard (rhodamine 6G) is measured. The diffusion time is related to r_0 through

$$\tau_{\mathrm{diff}} = \frac{r_0^{\,2}}{4D} \quad (3)$$

where D is the translational diffusion coefficient of the standard.

From the experimentally determined diffusion coefficient, an apparent hydrodynamic radius, R_h, can be calculated according to the Stokes−Einstein equation:

$$R_h = \frac{kT}{6\pi\eta D} \quad (4)$$

were k is the Boltzmann constant, T the absolute temperature, and η the viscosity of the solvent.

Experimental Setup. FCS measurements were performed with a ConfoCor fluorescence correlation spectrometer (Carl Zeiss Jena GmbH, Jena; EVOTEC Biosystems GmbH). The samples were excited using an Ar^+ laser. Excitation wavelengths of 514 nm were used. Fluorescence emission was detected between 520 and 610 nm.

For the determination of the binding constants, a mixture of TMR-Tf (with a concentration of 23 nM) was incubated with appropriate amounts of hTfR (between 1 nM and 2 μM binding sites) at room temperature, for at least 1 h. One hundred microliters of a sample solution was added to the chamber of a Lab-Tec chambered coverglass (NUNC GmbH, Wiesbaden, Germany), which was placed directly above the objective lens (C-Apochromat 40×/1.2 water immersion) through which the laser beam passes. The same objective lens serves for the collection of the fluorescence emission. Spectra were recorded for 30 s; each single measurement was repeated 10 times, and the results were averaged. The intensity fluctuations were analyzed by an autocorrelator board. Autocorrelation functions were automatically recorded on 288 channels, quasi-logarithmically spaced in time. These channels cover the dynamic range between 200 ns and 3438 s. Note that a strict temperature control is usually not required, because the small fluctuations induced by moderate temperature changes can be neglected (*14*).

Prior to the experiments, the structure parameter was determined with a standard rhodamine 6G solution. For the diffusion coefficient of rhodamine 6G, a value of 2.8×10^{-10} $m^2\ s^{-1}$ (*18*) was used. The translational diffusion time

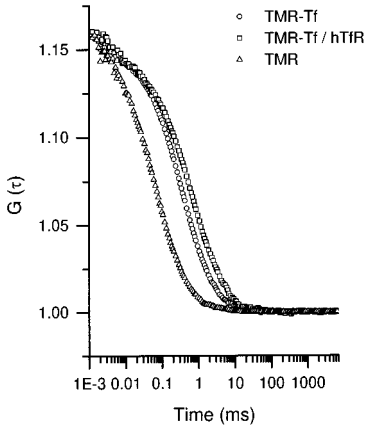

FIGURE 1: Fluorescence autocorrelation functions $G(\tau)$ as a function of the channel time for the translational diffusion of TMR (23 nM), TMR-Tf (23 nM), and hTfR (1.2 μM) labeled with TMR-Tf (23 nM). All experiments were performed in PBS with 150 mM NaCl at pH 7.5 and room temperature. The confocal volume was approximately 4×10^{-16} L.

constants of free TMR, free TMR-Tf, and TMR-Tf−hTfR were measured in independent experiments and served as input parameters for further fit procedures. According to eq 1, the relative concentration fraction of bound TMR-Tf (Y) and the amount (T), the diffusion time of triplet states (τ_T), and the total number of fluorescent species (N) served as free parameters. Spectra were sampled for 30 s, and each single measurement was repeated 10 times.

For measurements of association kinetics, the reaction was started by adding 90 μL of a hTfR solution to 10 μL of a TMR-Tf solution with the appropriate concentration to maintain pseudo-first-order conditions with respect to hTfR. Data recording was initiated directly after mixing the two solutions. All kinetics were observed at least for 50 min, and the correlation time was 30 s for each data point throughout.

Prior to the dissociation exchange kinetic experiments, the TMR-Tf−hTfR complex was formed by mixing hTfR with a stoichiometric ratio of 2:1 between TMR-Tf and hTfR, assuming that each hTfR dimer possesses two binding sites for Tf. After incubation for 60 min, no free TMR-Tf could be detected by fitting the autocorrelation functions to eq 1. The experiments were started by mixing a solution containing 23 nM complex with solutions containing different concentrations of unlabeled transferrin. Again, data recording was started immediately after mixing of the two components. Kinetics were observed for 50 min, with a correlation time of 30 s per data point.

Isothermal Titration Calorimetry (ITC)

ITC experiments of ligand binding to hTfR were performed in PBS by using the OMEGA high-sensitive microcalorimeter manufactured by MicroCal Inc. (Northampton, MA). A detailed description of the design and operation of this instrument has been provided previously (*20*). For measurements of the heat production accompanying the binding of Tf to hTfR, the receptor was loaded into the sample cell of the calorimeter (volume of 1.3592 mL) with a concentration of 4.4 mg/mL, and the reference cell was filled with distilled water. A solution of 40.7 mg/mL Tf was added to a 250 μL syringe. The system was allowed to equilibrate until a stable baseline was observed, before an automated titration was initiated. A typical experiment involved 13 injections of 7 μL of a Tf solution into the sample cell at time intervals of 3 min. Throughout the titration, the contents of the cell were stirred continuously at 400 revolutions/min. The data were evaluated to determine the enthalpy change H_b by integration of the whole energy production curve for each injection.

Table 1: Translational Diffusion Times (τ_{diff}), Diffusion Coefficients (D), and Hydrodynamic Radii (R_h) of All Investigated Species[a]

	τ_{diff} (ms)	D (m^2/s)	R_h (nm)
TMR	0.0581	2.88×10^{-10}	0.76
TMR-Tf	0.3048	4.13×10^{-11}	3.97
TMR-Tf−hTfR	1.0456	1.6×10^{-11}	13.6

[a] The experiments were carried out in 10 mM PBS at pH 7.5 and 298 K. The confocal volume was 6.37×10^{-16} L. For the diffusion time of rhodamine 6G, a value of 0.0598 ms was determined; therefore, the structure parameter is 5.853. A 30-fold excess of hTfR over TMR-Tf was used to determine the translational diffusion times of the complexes.

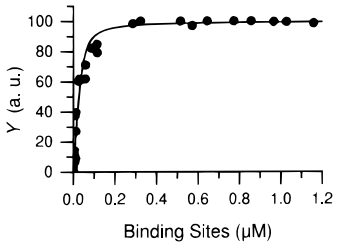

FIGURE 2: Equilibrium binding of TMR-Tf to hTfR. The Tf-TMR concentration was 23 nM. The relative amount of complex formed (Y) is plotted vs the concentration of binding sites. Nonlinear fit yields for the dissociation constants of the complex a value 7 nM.

RESULTS

In Figure 1, typical autocorrelation functions for TMR, TMR-Tf, and TMR-Tf−hTfR are displayed. All species exhibit autocorrelation functions consistent with their increasing molar mass. From the autocorrelation functions, only three components can be determined reliably. In every experiment, there is at least free labeled transferrin and complex detectable. To improve the signal-to-noise ratio, it is essential to reduce the amount of free dye to a minimum. For the detection of different fluorescent species, a mass ratio of at least 1:7 (Customer Support, EVOTEC GmbH, personal communication) is required. Therefore, mono-, bi-, and multiliganded receptor molecules cannot be distinguished and count as one fluorescent species. D and R_h for free dye, labeled transferrin, and the complex between labeled transferrin and hTfR, calculated according to eqs 3 and 5, are given in Table 1.

Figure 2 shows the binding curves for titration of TMR-labeled transferrin with increasing concentrations of hTfR. For the determination of dissociation constants, the fraction of bound ligand, Y, is measured at a constant concentration of TMR-TF as a function of the concentration of receptor hTfR. The fraction of bound ligand TMR-TF−hTfR is then plotted against the receptor concentration, and the data are described by a nonlinear regression model for the binding

of TMR-Tf to equal and independent binding sites according to:

$$Y = F\left\{\left(\frac{K_D + [\text{hTfR}] + [\text{TMR-Tf}]}{2}\right) - \sqrt{\left(\frac{K_D + [\text{hTfR}] + [\text{TMR-Tf}]}{2}\right)^2 - [\text{TMR-Tf}][\text{hTfR}]}\right\} \quad (5)$$

where F denotes a proportionality constant and K_D the dissociation constant. Note that in eq 5 the equilibrium concentration of the complex is expressed according to the mass action law.

The data are consistent with a binding of TMR-Tf to equal and independent binding sites on hTfR. For the dissociation constant, K_D, values of 7.0 ± 3.3 nM for the TMR-Tf−hTfR complex were obtained.

To determine kinetic constants for the complex formation, the decrease of the fraction of free ligand ($1 - Y$) was measured as a function of time, at a fixed concentration of TMR-Tf and varying concentrations of receptor under pseudo-first-order conditions (excess receptor). The fraction of free TMR-Tf was plotted against time. The monoexponential decay curves were interpreted by means of nonlinear regression with the following model:

$$(1 - Y)_t = A_0 \exp(t/\tau) + C \quad (6)$$

where A_0 is an amplitude and C denotes a constant offset. Here τ denotes the relaxation time of the reaction, not to be confused with the translational diffusion time constant τ_{diff}.

In Figure 3A, a typical decay curve is shown. The fraction of free TMR-Tf decreases monoexponentially with time, whereas the fraction of complex increases accordingly (data not shown). We observed a linear dependence between the reciprocal relaxation time, $1/\tau$, and the concentration of free receptor (Figure 4), which is characteristic for a reversible bimolecular binding reaction between the receptor and its ligand, according to

$$1/\tau = k_{-1} + k_{+1}[\text{hTfR}] \quad (7)$$

The association and dissociation rate constants (k_{+1} and k_{-1}, respectively) can be determined from the slope and intercept of the graph of the reciprocal relaxation times versus the concentration of free binding sites. They are estimated as follows: $k_{+1} = (1.1 \pm 0.1) \times 10^4\ s^{-1}\ M^{-1}$ and $k_{-1} = (6 \pm 4) \times 10^{-4}\ s^{-1}$.

The corresponding autocorrelation functions for the decay curve displayed in Figure 3A are shown in Figure 3B. The observed differences between the autocorrelation functions are compatible with TMR-Tf−hTfR complex formation. The small increase of the amplitude of $G(\tau)$ is possibly caused by an increase in the quantum yield of TMR-Tf upon binding. In static fluorescence titration experiments, we observed an increase of the fluorescence intensity, approximately 10%, associated with the binding of TMR-Tf to hTfR. However, the small increase in quantum yield was neglected during the further evaluation.

Two dissociation exchange kinetics at different unlabeled Tf concentrations are displayed in Figure 5. In this experiment, a large excess of unlabeled Tf was added to TMR-Tf−hTfR at a defined concentration. The decrease of the fraction of labeled complexes with time was recorded.

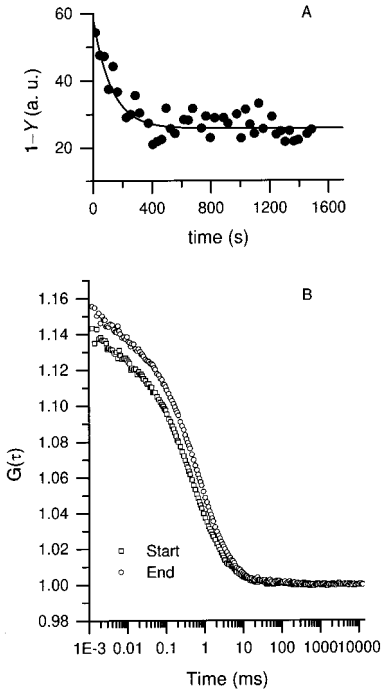

FIGURE 3: (A) Monoexponential decrease of the relative amount of free TMR-Tf ($1 - Y$) due to complex formation with hTfR. The hTfR concentration was 0.7 μM, and the TMR-Tf concentration was 23 nM. The experiment was started by mixing the hTfR solution with TMR-Tf. The time course of the reaction was followed until no further change occurred. The reciprocal relaxation time, $1/\tau$, for this experiment was determined to be $8 \times 10^{-3}\ s^{-1}$. Autocorrelation functions for the reaction of TMR-Tf with hTfR corresponding to $t = 0$ and 24.75 min are displayed in panel B.

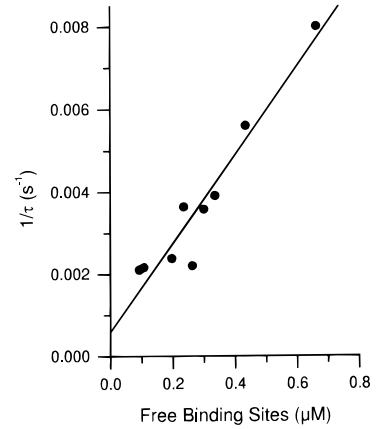

FIGURE 4: Linear relationship between the reciprocal relaxation times for the complex formation and the concentration of free hTfR binding sites. The association and dissociation rate constants were estimated from the slope and intercept of the graph: $k_{+1} = (1.1 \pm 0.1) \times 10^4\ s^{-1}\ M^{-1}$ and $k_{-1} = (6 \pm 4) \times 10^{-4}\ s^{-1}$.

The data for the dissociation exchange experiment gave a double-exponential decay curve for the fraction of labeled complex, Y, to which the following model was fitted:

$$Y = A_1 \exp\left(-\frac{t}{\tau_1}\right) + A_2 \exp\left(-\frac{t}{\tau_2}\right) \quad (8)$$

In Table 2, the amplitudes and relaxation times for typical experiments are shown.

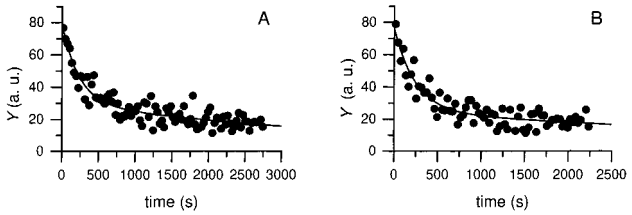

FIGURE 5: Dissociation exchange kinetics for two different concentrations of unlabeled Tf. The unlabeled Tf was added to a solution containing TMR-Tf−hTfR. The concentrations of unlabeled Tf were 296 (A) and 5.9 μM (B). There is no significant difference between the two reciprocal relaxation times for both reactions (see Table 2). The double-exponential fit gave χ^2 values of 24.5 (A) and 28.65 (B), whereas a single-exponential fit yielded χ^2 values of 55.4 (A) and 61.79 (B). Therefore, the description of the data by a biphasic dissociation exchange kinetics seems reasonable.

Table 2: Dissociation Exchange Kinetics, Amplitudes, and Relaxation Times[a]

[Tf] (μM)	A_1 (%)	$1/\tau_1$ (s^{-1})	A_2 (%)	$1/\tau_2$ (s^{-1})
296	48.2	4.3×10^{-3}	30.4	2.2×10^{-4}
118	43.2	3.7×10^{-3}	24.1	2.1×10^{-4}
39	44.5	4.6×10^{-3}	26.0	3.5×10^{-4}
6	51.0	4.1×10^{-3}	24.9	1.6×10^{-4}

[a] The experiments were carried out in 23 nM TMR-Tf−hTfR complex at 298 K.

We obtained biphasic decay curves for the dissociation of the TMR-Tf−hTfR complex. The exchange rate did not depend on the concentration of unlabeled transferrin.

Isothermal titration calorimetry (ITC) experiments for the binding of Tf to hTfR yield a constant amount of heat evolved per mole for each injection of Tf (Figure 6). For 13 injections of a concentrated Tf solution into a solution of 4.4 mg/mL hTfR (1.3592 mL), an exothermic enthalpy change ΔH of −49.2 kJ/mol was observed. The injection of a Tf solution in PBS shows a positive ΔH of 4.8 kJ/mol which was subtracted from the enthalpy change associated with the binding reaction of Tf and hTfR. Finally, the enthalpy change ΔH for the binding of Tf to hTfR was determined to be 44.4 kJ/mol. From ΔH and K_D, the other thermodynamic parameters can be calculated according to

$$\Delta G = -RT \ln 1/K_D$$

and

$$\Delta S = \frac{\Delta H - \Delta G}{T} \qquad (9)$$

According to these equations, the complex formation is associated with a free energy change of −46.5 kJ/mol and an entropy change of 7.1 J K^{-1} mol^{-1}.

DISCUSSION

In a solution containing 1% Triton X-100, hTfR exists mainly in a solubilized form as a dimer (*1*). In the absence of Triton X-100, hTfR forms associates, made up of 8−12 dimers (*6*). In detergent free solution, the mass difference between hTfR and Tf is high enough to enable FCS measurements. FCS allows the distinction between free dye, labeled transferrin, and the complex between transferrin and hTfR in solution. From the autocorrelation functions, the fraction of labeled Tf bound to hTfR can be obtained. It is not possible to discriminate mono-, bi-, and multiliganded hTfR associates. On the basis of these experiments, a common mechanism for complex formation in solution can be derived.

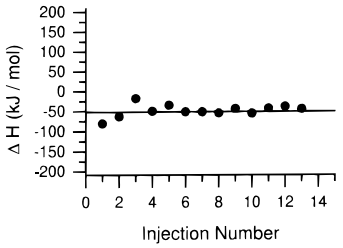

FIGURE 6: Isothermal titration calorimetry (ITC) experiment for the binding of Tf to hTfR. The heat evolved per mole of injected Tf is constant over 13 injections of 7 μL of 40.7 mg/mL Tf in 4.4 mg/mL hTfR. The experiment was conducted in PBS at pH 7.5 and 298 K. ΔH for the binding reaction is −49.2 kJ/mol. This value must be corrected for the heat of dilution of Tf (see the text).

As is evident from Figure 2, the fraction of labeled Tf bound to hTfR shows a dependence on the hTfR concentration typical for binding of Tf to equal and independent sites on the hTfR associate. The dissociation constant, determined using TMR-Tf as the ligand, equals 7 ± 3 nM which is in good agreement with the previously reported value of 5 nM, determined with purified, CHAPS-solubilized receptor using a radioimmunoassay (*11*, *21*). This close similarity between our dissociation constant and the literature data implies that the binding sites in detergent free solution are mainly located on the surface of the associates and are equally accessible from the bulk solution. This supports a structure model for the associates, where the hydrophobic membrane-spanning domains of the hTfR dimers are buried inside the particle, while the hydrophilic parts, including the binding domains, are in contact with the aqueous environment. However, radioimmunoassay-based methods provide no means for the determination of rate constants. Further, in the case of solid phase assays the properties of the surfaces, e.g., diffusion potentials, and their interaction with the receptor are usually neglected.

The association kinetics yielded monoexponential decay curves for the fraction of free TMR-Tf due to complex formation (Figure 3). The reciprocal relaxation time, $1/\tau$, is a linear function of the hTfR concentration. This relationship is compatible with a bimolecular reversible binding reaction between TMR-Tf and equal and independent sites on hTfR associates according to

$$\text{TMR-Tf} + \text{hTfR} \underset{k_{-1}}{\overset{k_{+1}}{\rightleftharpoons}} \text{TMR-Tf−hTfR}$$

Association and dissociation rate constants (k_{+1} and k_{-1}, respectively) of (1.1 ± 0.1) × 10^4 s^{-1} M^{-1} and (6 ± 4) × 10^{-4} s^{-1} were determined from a graph of the reciprocal relaxation time as function of hTfR concentration (Figure 4). The ratio between k_{-1} and k_{+1} gives a dissociation constant K_D of 55 ± 41 nM. The deviation from the previously determined value and also the large error are due to the imprecise estimate for the very small dissociation rate constant k_{-1}.

For a simple diffusion-controlled binding reaction, a typical value for k_{+1} is 10^8 s^{-1} M^{-1}. Our association rate constant

is 4 orders of magnitude lower than this expected value. This is probably due to isomerization or rearrangement steps limiting the overall reaction rate.

For the kinetic constants that were determined, no reference data are available. Rauer et al. (*22*) observed in FCS experiments a slightly lower association rate constant, for binding of TMR-labeled bungarotoxin to acetylcholine receptor, compared with the k_{+1} obtained with unlabeled bungarotoxin. They interpreted this difference in terms of steric hindrance. We cannot exclude such effects for our system. Overall, the interpretation of the association kinetics under pseudo-first-order conditions seems reasonable. We observed a linear relationship between the rate constants and the concentration of hTfR binding sites. Only a reversible bimolecular reaction displays under this conditions such a behavior.

The interpretation of the dissociation exchange kinetics is much more difficult. We observed no concentration dependence and obviously biexponential decay curves for the decrease of the relative amount of complex between TMR-Tf and hTfR in the presence of a large excess of unlabeled Tf. To explain this behavior, we suggest a mechanism involving two different conformational states of hTfR, according to the following reaction scheme involving six different states. Tf is assumed to be able to bind to both conformations of hTfR, and the rate constant of dissociation of Tf from hTfR is assumed to be dependent on its conformation. We, therefore, considered two possible pathways for the replacement of TMR-Tf by Tf:

$$\text{hTfR}' \rightleftarrows \text{hTfR}''$$

$$\text{TMR-Tf}-\text{hTfR}' \underset{k'_{+1}}{\overset{k'_{-1}}{\rightleftharpoons}} \text{hTfR}' + \text{TMR-Tf},\ \text{hTfR}' + \text{Tf} \underset{k'_{-2}}{\overset{k'_{+2}}{\rightleftharpoons}} \text{Tf}-\text{hTfR}' \quad \text{(I)}$$

$$\text{TMR-Tf}-\text{hTfR}'' \underset{k''_{+1}}{\overset{k''_{-1}}{\rightleftharpoons}} \text{hTfR}'' + \text{TMR-Tf},\ \text{hTfR}'' + \text{Tf} \underset{k''_{-2}}{\overset{k''_{+2}}{\rightleftharpoons}} \text{Tf}-\text{hTfR}' \quad \text{(II)}$$

A kinetic analysis (*23*) yields for expression I

$$\frac{1}{\tau'} = \dot{k}_{-1} + \dot{k}_{-2} \tag{10}$$

with

$$\dot{k}_{-1} = \frac{k'_{-1}}{1 + \dfrac{k'_{+1}[\text{TMR-Tf}]}{k'_{+2}[\text{Tf}]}}$$

and

$$\dot{k}_{-2} = \frac{k'_{-2}}{1 + \left(\dfrac{k'_{+2}[\text{Tf}]}{k'_{+1}[\text{TMR-Tf}]}\right)}$$

Under the condition where [Tf] ≫ [TMR-Tf] and $k'_{+1} \approx k'_{+2}$, eq 10 reduces to $1/\tau' = k'_{-1}$. For reaction II, the same approximation holds, where $1/\tau'' = k''_{-1}$.

This reaction scheme accounts for the biexponential behavior of the plots in Figure 5, and the independence of the dissociation exchange kinetics from the unlabeled Tf concentration can be explained. A model in which the binding of unlabeled Tf is rate-determining can be excluded, since this would be expected to show an increase in rate with increasing Tf concentrations. In the model presented above, the reaction rate is only dependent on the dissociation of TMR-Tf from the complex. It should be noted, however, that a model in which the TMR-Tf−hTfR complex undergoes a slow conformational change prior to the release of TMR-Tf is also feasible:

$$\text{TMR-Tf}-\text{hTFR}'' \rightleftarrows \text{TMR-Tf}-\text{hTfR}' \underset{k'_{+1}}{\overset{k'_{-1}}{\rightleftharpoons}} \text{hTfR}' + \text{TMR-Tf}$$

$$\text{hTfR}' + \text{Tf} \rightleftarrows \text{TF}-\text{hTfR}'$$

The fast kinetic phase would then be attributed to the release of TMR-Tf directly from the hTfR′ conformation, whereas the slow kinetic phase is attributed to release from the hTfR′ conformation only after a slower conformational change from hTfR″. This mechanism is, however, mathematically indistinguishable from that shown above under pathways I and II. In fact, it is only a special case of them, in which it is assumed that TMR-Tf is incapable of directly dissociating from the hTfR″ conformation.

For the dissociation exchange kinetics, two dissociation rate constants could be determined. If we assume that the association rate constant (Figure 4) ($k_{+1} = 1.1 \times 10^4$ s^{-1} M^{-1}) is equal for both reactions I and II, two equilibrium constants (K_D) of 20 and 400 nM can be calculated with the dissociation rate constants displayed in Table 2. The higher constant could not be detected directly in equilibrium FCS measurements (Figure 2).

In addition to kinetic parameters of the interaction between Tf and hTfR, we determined the basic thermodynamic constants describing the complex formation. From the experimentally determined binding constant and the enthalpy change associated with the binding process, the free energy change and the change of the entropy could be calculated. We measured in ITC experiments an enthalpy change of −44.4 kJ/mol which is similar to the free energy change of −46.5 kJ/mol for the binding reaction. Therefore, the entropy change is very small, but still positive. We thus conclude that the reaction is mainly enthalpy driven. This suggests that the major factor determining the stability of the transferrin−transferrin receptor complex is the formation of specific noncovalent bonds between the two partners rather than the accompanying change in solvation, since the latter would be the driving force for a hydrophobic interaction involving a significant entropy change.

ACKNOWLEDGMENT

We thank Dr. Ronald Clarke (MPI für Biophysik, Frankfurt/Main, Germany) for valuable discussions concerning the reaction mechanisms. We also thank Prof. Dr. J. F. Holzwarth (Fritz Haber Institut, Berlin, Germany) for providing us with the facilities for ITC measurements. The support by the staff of the maternity ward, Frauen-und Polyklinik, Charité Campus Virchow Klinikum, Berlin, is deeply acknowledged.

REFERENCES

1. Turkewitz, A. P., Amatruda, J. F., Borhani, D., Harrison, S. C., and Schwartz, A. L. (1988) *J. Biol. Chem. 263*, 8318−8325.
2. McClelland, A., Kühn, L. C., and Ruddle, F. H. (1984) *Cell 39*, 274−276.
3. Enns, C. A., and Sussman, H. H. (1981) *J. Biol. Chem. 256*, 9820−9823.
4. Omary, M. B., and Trowbridge, I. S. (1981) *J. Biol. Chem. 256*, 12888−12892.
5. Schneider, C., Sutherland, R., Newman, R., and Greaves, M. (1982) *J. Biol. Chem. 257*, 8516−8522.
6. Fuchs, H., Gessner, R., Tauber, R., and Ghosh, R. (1995) *Biochemistry 34*, 6196−6207.
7. Brown, P. J., Molloy, C. M., and Johnson, P. M. (1982) *Placenta 3*, 21−28.
8. Shindelman, J. E., Ortmeyer, A. E., and Sussman, H. H. (1981) *Int. J. Cancer 27*, 329−334.
9. Tsunoo, H., and Sussman, H. H. (1983) *J. Biol. Chem. 258*, 4118−4122.
10. Chitambar, C. R., and Zivkovic, Z. (1989) *Blood 74*, 602−608.
11. Kanevsky, V. Yu., Pozdnyakova, L. P., Katukov, V. Yu., and Severin, S. E. (1997) *Biochem. Mol. Biol. Int. 42*, 309−314.
12. EVOTEC GmbH (1995) *Physikochemische Betrachtungen zur FCS-Analytik*, Hamburg, Germany.
13. Elson, E. L., and Magde, D. (1974) *Biopolymers 13*, 1−27.
14. Magde, D., Elson, E. L., and Webb, W. W. (1974) *Biopolymers 13*, 29−61.
15. Magde, D., Webb, W. W., and Elson, E. L. (1978) *Biopolymers 17*, 361−376.
16. Eigen, M., and Rigler, R. (1994) *Proc. Natl. Acad. Sci. U.S.A. 91*, 5740−5747.
17. Rigler, R. (1995) *J. Biotechnol. 41*, 177−186.
18. Rigler, R., Mets, Ü., Widengren, J., and Kask, P. (1993) *Eur. Biophys. J. 22*, 169−175.
19. Meyer-Almes, F. J., Wyzgoll, K., and Powell, M. J. (1998) *Biophys. Chem. 75*, 151−160.
20. Wiseman, T., Williston, S., Brandts, J. F., and Lin, L.-N. (1989) *Anal. Biochem. 179*, 131−137.
21. Anderson, G. J., Mackerras, A., Powell, L. W., and Halliday, J. W. (1986) *Biochim. Biophys. Acta 884*, 225−233.
22. Rauer, B., Neumann, E., Widengren, J., and Rigler, R. (1996) *Biophys. Chem. 58*, 3−12.
23. Gutfreund, H. (1995) *Kinetics for the Life Sciences*, Cambridge University Press, Cambridge, U.K.

BI9819576